

Modification of generalized vector form factors and transverse charge densities of the nucleon in nuclear matter

Ju-Hyun Jung,^{1,2,*} Ulugbek Yakhshiev,^{1,†} and Hyun-Chul Kim^{1,3,‡}

¹*Department of Physics, Inha University, Incheon 22212, Republic of Korea*

²*Institute of Physics, University of Graz, Universitätsplatz 5, A-8010 Graz, Austria*

³*School of Physics, Korea Institute for Advanced Study (KIAS), Seoul 02455, Republic of Korea*

(Received 23 December 2015; published 9 March 2016)

We investigate the medium modification of the generalized vector form factors of the nucleon, which include the electromagnetic and energy-momentum tensor form factors, based on an in-medium modified π - ρ - ω soliton model. We find that the vector form factors of the nucleon in nuclear matter fall off faster than those in free space, which implies that the charge radii of the nucleon become larger in nuclear medium than in free space. We also compute the corresponding transverse charge densities of the nucleon in nuclear matter, which clearly reveal the increasing of the nucleon size in nuclear medium.

DOI: [10.1103/PhysRevD.93.054016](https://doi.org/10.1103/PhysRevD.93.054016)

I. INTRODUCTION

Understanding the electromagnetic form factors (EMFFs) of the nucleon has been one of the most important issues in hadronic physics, since they reveal the internal quark structure of the nucleon. While the EMFFs of the nucleon have been studied well over several decades, their precise data were obtained only recently by measuring the transverse and longitudinal recoil proton polarizations [1–11]. These new experimental data have drawn a great deal of attention both experimentally and theoretically (see recent reviews and references therein [12–15]). In the meanwhile, form factors of the nucleon can be defined as Mellin moments of the corresponding generalized parton distributions (GPDs) that unveil novel aspects of the internal structure of the nucleon [16–19] (see also the following reviews [20–22]). This new definition of the form factors enables one to get access to the energy-momentum tensor form factors (EMTFFs) and the tensor form factors via the GPDs, which cannot be otherwise directly measured experimentally. In this definition, the energy-momentum tensor form factors can be also understood as the second Mellin moments of the isoscalar vector GPDs of the nucleon.

The Fourier transforms of the generalized vector form factors of the nucleon including the EMFFs and the EMTFFs in the transverse plane, as viewed from a light front frame moving toward a nucleon, makes it possible to see how the charge densities of quarks are distributed transversely [23,24]. These are called transverse charge densities and they provide correctly a probability of finding quarks inside a nucleon in the transverse plane. Transverse charge densities inside both the unpolarized and polarized

nucleons have been already investigated within empirical methods [25,26] and specific models [27–30].

Furthermore, it is of equal importance to examine how the EM structure of the nucleon is changed in nuclear matter. Studying the EMFFs of the nucleon in nuclear medium provides a new perspective on EM properties of the nucleon modified in nuclei [31–39]. In fact, the first experimental study of deeply virtual Compton scattering on (gaseous) nuclear targets (H, He, N, Ne, Kr, Xe) was reported in Ref. [40]. While uncertainties of the first measurement are so large that one is not able to observe nuclear modifications of the nucleon structure, future experiments will provide more information on medium modifications of the EM properties of the nucleons.

In the present work, we want to investigate the nucleon EMFFs and the transverse charge densities of quarks inside a nucleon in nuclear matter within the framework of an in-medium modified soliton model with explicit π - ρ - ω degrees of freedom. The model has certain virtues: it is simple but respects the chiral symmetry and its spontaneous breaking. Moreover, one can easily extend it including the influence of the surrounding nuclear environment to the nucleon properties based on modifications of the meson properties in nuclear medium [41,42]. In this context, the EMTFFs of the nucleon, which are yet another of the fundamental form factors that are related to the generalized EMFFs, have been investigated in free space [43,44] and in nuclear matter within the chiral soliton approaches [45,46]. The results have explained certain interesting features of the modifications of nucleon properties in nuclear matter such as the pressure and angular momentum. Indeed, we will also show in this work how the EM properties of the nucleon are changed in nuclear matter in a simple manner. We will also see that the transverse charge densities expose noticeably how the distribution of quarks undergo changes in the presence of nuclear medium.

*juhyun@inha.edu

†yakhshiev@inha.ac.kr

‡hchkim@inha.ac.kr

The present paper is organized as follows: In Sec. II, we briefly explain the general formalism of the π - ρ - ω soliton model modified in nuclear medium. In Sec. III, we describe how one can compute the generalized vector form factors within this framework. In Sec. IV, we present the results from the present work and discuss them. The final section is devoted to the summary and the conclusion.

II. GENERAL FORMALISM

We start from the in-medium modified effective chiral Lagrangian with the π , ρ , and ω meson degrees of freedom, where the nucleon arises as a topological soliton [47]. The Lagrangian has the form

$$\mathcal{L}^* = \mathcal{L}_\pi^* + \mathcal{L}_V^* + \mathcal{L}_{\text{kin}}^* + \mathcal{L}_{\text{WZ}}^*, \quad (1)$$

where the corresponding terms are expressed as

$$\begin{aligned} \mathcal{L}_\pi^* &= \frac{f_\pi^2}{4} \text{Tr}(\partial_0 U \partial_0 U^\dagger) - \alpha_p \frac{f_\pi^2}{4} \text{Tr}(\partial_i U \partial_i U^\dagger) \\ &+ \alpha_s \frac{f_\pi^2 m_\pi^2}{2} \text{Tr}(U - 1), \end{aligned} \quad (2)$$

$$\mathcal{L}_V^* = \frac{f_\pi^2}{2} \text{Tr}[D_\mu \xi \cdot \xi^\dagger + D_\mu \xi^\dagger \cdot \xi]^2, \quad (3)$$

$$\mathcal{L}_{\text{kin}}^* = -\frac{1}{2g_V^2 \zeta_V} \text{Tr}(F_{\mu\nu}^2), \quad (4)$$

$$\begin{aligned} \mathcal{L}_{\text{WZ}}^* &= \left(\frac{N_c}{2} g_\omega \sqrt{\zeta_\omega} \right) \omega_\mu \frac{\epsilon^{\mu\nu\alpha\beta}}{24\pi^2} \\ &\times \text{Tr}\{(U^\dagger \partial_\nu U)(U^\dagger \partial_\alpha U)(U^\dagger \partial_\beta U)\}. \end{aligned} \quad (5)$$

Here the asterisk designates medium modified quantities. The SU(2) chiral field is written as $U = \xi_L^\dagger \xi_R$ in unitary gauge, and the field-strength tensor and the covariant derivative are defined, respectively, as

$$F_{\mu\nu} = \partial_\mu V_\nu - \partial_\nu V_\mu - i[V_\mu, V_\nu], \quad (6)$$

$$D_\mu \xi_{L(R)} = \partial_\mu \xi_{L(R)} - iV_\mu \xi_{L(R)}, \quad (7)$$

where the vector field V_μ includes the ρ -meson and ω -meson fields, i.e. ρ_μ and ω_μ , respectively, expressed as

$$V_\mu = \frac{g_V \sqrt{\zeta_V}}{2} (\boldsymbol{\tau} \cdot \boldsymbol{\rho}_\mu + \omega_\mu) \quad (8)$$

with the Pauli matrices $\boldsymbol{\tau}$ in isospin space.

Note that in Eqs. (3), (4), and (8) the subscript V generically stands for both the ρ -meson and the ω -meson and for compactness we keep the generic form of those expressions. One can separate Eqs. (3) and (4) into the ρ - and ω -meson parts using the definitions (6), (7), and (8).

Then g_V designates g_ρ for the ρ meson or g_ω for the ω . $N_c = 3$ is the number of colors.

The input parameters of the model in Eqs. (2)–(5) can be classified into two different classes: the parameters f_π , m_π , g_ρ , g_ω , and N_c are related to the corresponding observables in free space, while α_p , α_s , and ζ_V are pertinent to properties of pionic atoms and infinite and homogenous nuclear matter.¹

In free space, in-medium parameters are all set equal to one: $\alpha_p = \alpha_s = \zeta_\omega = \zeta_\rho = 1$ and the other parameters are fixed by using either experimental or empirical data on the pion and the vector mesons [48]. The pion decay constant and mass are taken to be $f_\pi = 93$ MeV and $m_\pi = 135$ MeV (the neutral pion mass). The values of the coupling constants for the ρ and ω mesons are given respectively as $g_\rho = 5.86$ and $g_\omega = 5.95$. The Kawarabayashi-Suzuki–Riazuddin-Fayyazuddin (KSRF) relation connects them to the masses of the vector mesons, i.e. $m_\rho = 770$ MeV and $m_\omega = 782$ MeV, as follows

$$2f_\pi^2 g_\rho^2 = m_\rho^2, \quad 2f_\pi^2 g_\omega^2 = m_\omega^2. \quad (9)$$

In general, the parameters α_p , α_s , and ζ_V stand for the medium functionals which are the essential quantities in the present work. They depend on the nuclear matter density ρ and are defined as

$$\begin{aligned} \alpha_p(\rho) &= 1 - \frac{4\pi c_0 \rho / \eta}{1 + g_0' 4\pi c_0 \rho / \eta}, \\ \alpha_s(\rho) &= 1 - 4\pi \eta b_0 \rho m_\pi^{-2}, \\ \zeta_V(\rho) &= \exp \left\{ -\frac{\gamma_{\text{num}} \rho}{1 + \gamma_{\text{den}} \rho} \right\}. \end{aligned} \quad (10)$$

They provide crucial information on how the nuclear-matter environment influences properties of the single soliton [47]. The η is a kinematic factor defined as $\eta = 1 + m_\pi / m_N \approx 1.14$. The values of the empirical parameters $b_0 = -0.024 m_\pi^{-1}$ and $c_0 = 0.09 m_\pi^{-3}$ are taken from the analysis of pionic atoms and the data on low-energy pion-nucleus scattering. The $g_0' = 0.7$ denotes the Lorentz-Lorenz factor that takes into account the short-range correlations [49].

The additional parameters γ_{num} and γ_{den} are introduced phenomenologically to reproduce the saturation point at normal nuclear matter. Two different models have been discussed in the framework of the present approach [47], in order to introduce a nuclear modification in the present soliton approach, which we will briefly explain here. In *Model I*, one neglects the small mass difference of the ρ and ω mesons in free space ($m_\omega = m_\rho = 770$ MeV,

¹ ζ_V denotes also a generic form for both ζ_ρ and ζ_ω which appear in the corresponding ρ - and ω -meson parts of the Lagrangian.

$g_\omega = g_\rho = 5.86$) and assumes that the KSRF relation still holds in nuclear matter

$$2f_\pi^2 g_\rho^2 \zeta_\rho = m_\rho^{*2} = m_\omega^{*2}, \quad \zeta_\rho = \zeta_\omega \neq 1. \quad (11)$$

In *Model II*, on the other hand, we remove the degeneracy of the vector meson masses in free space ($m_\rho \neq m_\omega = 782$ MeV, $g_\rho \neq g_\omega = 5.95$), and instead of Eq. (11) assume that the KSRF relation is valid only for the ρ meson, with the ω meson kept as in free space:

$$2f_\pi^2 g_\rho^2 \zeta_\rho = m_\rho^{*2} \neq m_\omega^{*2}, \quad \zeta_\rho \neq 1, \quad \zeta_\omega = 1. \quad (12)$$

These two different models are devised to implement possible ways of nuclear modification. We take into account the possibility that the ρ and ω meson degrees of freedom could respond differently to a nuclear environment [50,51]. The effects of the ω -mesons are mainly limited to the inner core of the nucleon. Therefore, the two variants of the model describe the situation that the inner core of the nucleon is more (Model I) or less (Model II) affected by medium effects. The latter is a plausible scenario, at least around the normal nuclear matter density.

In practice, these two models yield comparable results in many respects. A notable (and in our context important) difference, however, is the description of the incompressibility of symmetric nuclear matter: Model I yields a smaller value of the incompressibility, while Model II produces a larger one. It means that Model II gives a stiffer nuclear binding energy and agrees better with the data (see explanations in Ref. [47]). In both models the values of γ_{num} and γ_{den} are fitted to reproduce the coefficient of the volume term in the empirical mass formula $a_V \approx 26$ MeV. Although this is larger than the experimental value $a_V^{\text{exp}} \approx 16$ MeV, the relative change of the in-medium nucleon mass is reproduced correctly (See Eq. (12) in Ref. [47] and the corresponding explanation.). In Model I we have $\gamma_{\text{num}} = 2.390m_\pi^{-3}$ and $\gamma_{\text{den}} = 1.172m_\pi^{-3}$, whereas in Model II we employ $\gamma_{\text{num}} = 1.970m_\pi^{-3}$ and $\gamma_{\text{den}} = 0.841m_\pi^{-3}$. For further details on these two models in relation to nuclear matter properties, and to the classical and quantum solution in free space and in nuclear matter we refer to Refs. [46,47]. In the next section we concentrate on generalized form factors and the corresponding transverse charge densities.

III. GENERALIZED VECTOR FORM FACTORS AND TRANSVERSE CHARGE DENSITIES

The generalized vector form factors of the nucleon can be defined as the matrix element of a vector operator as follows:

$$\begin{aligned} & \langle N(p', s) | \bar{\psi}(0) \gamma^{\{i} D^{\mu_1} \dots i D^{\mu_n\}} \psi(0) | N(p, s) \rangle \\ &= \bar{u}(p', s') \left[\sum_{i=0, \text{even}}^n \left\{ \gamma^{\{\mu} \Delta^{\mu_1} \dots \Delta^{\mu_i} P^{\mu_{i+1}} \dots P^{\mu_n\}} A_{n+1, i}(\Delta^2) \right. \right. \\ & \quad \left. \left. - i \frac{\Delta_\alpha \sigma^{\alpha\{\mu} \Delta^{\mu_1} \dots \Delta^{\mu_i} \bar{P}^{\mu_{i+1}} \dots \bar{P}^{\mu_n\}} B_{n+1, i}(\Delta^2) \right\} \right. \\ & \quad \left. + \frac{\Delta^\mu \Delta^{\mu_1} \dots \Delta^{\mu_n}}{M_N} C_{n+1, 0}(\Delta^2) \Big|_{\text{odd}} \right] u(p, s), \quad (13) \end{aligned}$$

where D_i^μ denotes the covariant operator in quantum chromodynamics (QCD) and the braces “{ }” stand for the symmetrization. Here Δ^{μ_i} and the P^{μ_i} are the momentum transfer and the average of the momenta defined respectively as $\Delta^{\mu_i} = p'^{\mu_i} - p^{\mu_i}$ and $P^{\mu_i} = (p'^{\mu_i} + p^{\mu_i})/2$; $u(p, s)$ and $\bar{u}(p', s')$ designate the spinor of the nucleon; $A_{n+1, i}(\Delta^2)$, $B_{n+1, i}(\Delta^2)$, and $C_{n+1, 0}(\Delta^2)$ represent the generalized vector form factors (GVFFs) that are related to the Mellin moments of the GPDs, which are given as

$$\begin{aligned} \int_{-1}^1 x^n H(x, \xi, t) &= \sum_{i=0, \text{even}}^n (-2\xi)^i A_{n+1, i}(\Delta^2) \\ & \quad + (-2\xi)^{n+1} C_{n+1, 0}(\Delta^2) \Big|_{n, \text{odd}}, \\ \int_{-1}^1 x^n E(x, \xi, t) &= \sum_{i=0, \text{even}}^n (-2\xi)^i B_{n+1, i}(\Delta^2) \\ & \quad - (-2\xi)^{n+1} C_{n+1, 0}(\Delta^2) \Big|_{n, \text{odd}}. \quad (14) \end{aligned}$$

Here $H(x, \xi, t)$ and $E(x, \xi, t)$ are the twist-2 vector GPDs. The usual Dirac and Pauli form factors are identified as the leading GVFFs:

$$F_1(\Delta^2) = A_{1, 0}(\Delta^2), \quad F_2 = B_{1, 0}(\Delta^2), \quad (15)$$

which are defined as the matrix element of the electromagnetic current:

$$\begin{aligned} & \langle N(p', s') | \bar{\psi}(0) \gamma_\mu \hat{Q} \psi(0) | N(p, s) \rangle \\ &= \bar{u}(p', s') \left[\gamma^\mu F_1(\Delta^2) + i \frac{\sigma^{\mu\nu} \Delta_\nu}{2M_N} F_2(\Delta^2) \right] u(p, s). \quad (16) \end{aligned}$$

The nucleon matrix elements of the symmetric EMT operator are parametrized in terms of the EMTEFFs as follows [17,52]:

$$\begin{aligned} & \langle N(p', s') | \hat{T}_{\mu\nu}(0) | N(p, s) \rangle \\ &= \bar{u}(p', s') \left[M_2(\Delta^2) \frac{P_\mu P_\nu}{M_N} \right. \\ & \quad \left. + J(\Delta^2) \frac{i(P_\mu \sigma_{\nu\rho} + P_\nu \sigma_{\mu\rho}) \Delta^\rho}{2M_N} \right. \\ & \quad \left. + d_1(\Delta^2) \frac{\Delta_\mu \Delta_\nu - \Delta_{\mu\nu} \Delta^2}{5M_N} \right] u(p, s). \quad (17) \end{aligned}$$

Similarly, the EMTFFs are related to the second moments of the vector GPDs and in a such way related to the GVFFs in the next-to-leading order (NLO) as follows:

$$\begin{aligned} A_{2,0}(\Delta^2) &= \int_{-1}^1 dx x H(x, 0, \Delta^2) = M_2(\Delta^2), \\ B_{2,0}(\Delta^2) &= \int_{-1}^1 dx x E(x, 0, t) = 2J(\Delta^2) - M_2(\Delta^2), \\ C_{2,0}(\Delta^2) &= \frac{1}{5} d_1(\Delta^2). \end{aligned} \quad (18)$$

In this work we want to examine the modification of the EMFFs and the EMTFFs of the nucleon in nuclear medium. Let us first consider the EMFFs of the nucleon. In the Breit frame one has $\Delta = (0, \mathbf{\Delta})$ and $\mathbf{p}' = -\mathbf{p}$. Since it is more convenient to introduce the positive definite square of the momentum transfer $Q^2 = -\Delta^2 > 0$ to describe the form factors, we will use it from now on. The Sachs EMFFs G_E and G_M of the nucleon are expressed in terms of the Dirac and Pauli form factors:

$$G_E(Q^2) = F_1(Q^2) + \frac{Q^2}{4M_N^2} F_2(Q^2) \quad (19)$$

$$G_E^V(Q^2) = \frac{4\pi}{\lambda^*} \int_0^\infty j_0(Qr) \left[\frac{f_\pi r^2}{3} \left\{ 4\sin^4 \frac{F}{2} + (1 + 2\cos F)\xi_1 + \xi_2 \right\} + \frac{g\sqrt{\xi}}{8\pi^2} \phi F' \sin^2 F \right] dr, \quad (24)$$

$$G_M^V(Q^2) = \frac{8\pi}{3} M_N \int_0^\infty r^2 \frac{j_1(Qr)}{Qr} \left[2f_\pi^2 \left(2\sin^4 \frac{F}{2} - 2(1 - \alpha_p) \frac{1}{4} \sin^2 F - G \cos F \right) + \frac{3g\sqrt{\xi}}{4\pi^2} \omega F' \sin^2 F \right], \quad (25)$$

where the detailed expressions for the profile functions, $\omega(r)$, $\phi(r)$, $F(r)$, $\xi_1(r)$, and $\xi_2(r)$, can be found in Ref. [47]. The proton and neutron EMFFs are expressed in terms of the isoscalar and isovector FFs

$$G_{E,M}^{p,n}(Q^2) = G_{E,M}^S(Q^2) + \tau_3 G_{E,M}^V(Q^2), \quad (26)$$

where τ_3 is the eigenvalue of $\hat{\tau}_3$ for a given nucleon isospin state. At the zero momentum transfer ($Q^2 = 0$) the EMFFs are normalized as

$$G_E^p(0) = 1, \quad G_E^n(0) = 0, \quad G_M^{p,n}(0) = \mu_{p,n}. \quad (27)$$

Since we already have studied the EMTFFs in nuclear matter within the present approach [46], we refer to Ref. [46] for details.

Once we obtain the EMFFs and the EMTFFs of the nucleon, we can proceed to derive the transverse quark charge densities inside a nucleon, which show how the charges and magnetizations of the quarks are distributed in the transverse plane inside a nucleon [23,53].

$$G_M(Q^2) = F_1(Q^2) + F_2(Q^2), \quad (20)$$

which can be represented respectively as the Fourier transforms of the charge and current densities

$$\begin{aligned} G_E(Q^2) &= \int d^3r e^{i\Delta \cdot r} J^0(r), \\ G_M(Q^2) &= m_N \int d^3r e^{i\Delta \cdot r} [\mathbf{r} \times \mathbf{J}(r)]_3. \end{aligned} \quad (21)$$

Here J^0 and \mathbf{J} denote respectively the charge and current densities. Note that the EM current J^μ is defined as the sum of the baryonic current B^μ and the third component of the isovector current \mathbf{V}^μ . The final expressions for the in-medium modified isoscalar and isovector FFs are derived as

$$G_E^S(Q^2) = -\frac{m_\omega^{*2}}{3\sqrt{\xi}g} \int_0^\infty r^2 j_0(Qr) \omega(r) dr, \quad (22)$$

$$G_M^S(Q^2) = -\frac{m_\omega^{*2}}{3\sqrt{\xi}g} \frac{M_N}{\lambda^*} 2\pi \int_0^\infty r^2 \frac{j_1(Qr)}{Qr} \phi(r) dr, \quad (23)$$

The transverse charge density inside an unpolarized nucleon is defined as the two-dimensional Fourier transform of the Dirac form factor:

$$\begin{aligned} \rho_{\text{ch}} &= \frac{1}{(2\pi)^2} \int d^2q e^{iq \cdot b} F_1(Q^2) = \int_0^\infty \frac{dQ}{2\pi} Q J_0(Qb) F_1(Q^2) \\ &= \int_0^\infty \frac{dQ}{2\pi} Q J_0(Qb) \frac{G_E(Q^2) + \tau G_M(Q^2)}{1 + \tau}, \end{aligned} \quad (28)$$

where b designates the impact parameter, i.e., the distance in the transverse plane to the place where the density is being probed, and J_0 denotes the Bessel function of order zero [25,54]. The anomalous magnetization density in the transverse plane [54,55] is defined as

$$\rho_{\text{m}} = -b \frac{d}{db} \rho_2(b) = b \int_0^\infty \frac{dQ}{2\pi} Q^2 J_1(Qb) F_2(Q^2), \quad (29)$$

where $\rho_2(b)$ is directly given by the two-dimensional Fourier transform of the Pauli form factor:

$$\rho_2(b) = \int_0^\infty \frac{dQ}{2\pi} Q J_0(Qb) F_2(Q^2). \quad (30)$$

Assume that the nucleon is transversely polarized along the x axis. Then the polarization of the nucleon can be expressed in terms of the transverse spin operator of the nucleon $\mathbf{S}_\perp = \cos \varphi_S \hat{e}_x + \sin \varphi_S \hat{e}_y$, so that the transverse charge density inside a transversely polarized nucleon is written as [26]

$$\rho_T(\mathbf{b}) = \rho_{\text{ch}} - \sin(\varphi_b - \varphi_S) \frac{1}{2M_N} \rho_m(b), \quad (31)$$

where the angle φ_b is defined in the position vector \mathbf{b} that stands for the impact parameter or the transverse distance from the center of the nucleon in the transverse plane $\mathbf{b} = b(\cos \varphi_b \hat{e}_x + \sin \varphi_b \hat{e}_y)$.

Since the EMFFFs are identified as the generalized vector FFs in the isoscalar channel, one can also define the transverse isoscalar densities in the case of the EMFFFs, which takes the following form:

$$\rho_{20}(b) = \int_0^\infty \frac{dQ}{2\pi} Q J_0(Qb) A_{2,0}(Q^2). \quad (32)$$

When the nucleon is polarized along the x axis in the transverse plane, the transverse isoscalar density inside the polarized nucleon is defined as

$$\begin{aligned} \rho_{20,T}(\mathbf{b}) &= \rho_{20}(b) - \sin(\phi_b - \phi_S) \\ &\times \int_0^\infty \frac{Q^2 dQ}{4\pi M_N} J_1(Qb) B_{2,0}(Q^2). \end{aligned} \quad (33)$$

IV. RESULTS AND DISCUSSIONS

In this section we present the numerical results of the form factors and related observables and discuss their physical implications.

A. Electromagnetic form factors and transverse charge densities

We first show the results for the traditional charge and magnetization radii and the magnetic moments of the proton and the neutron. Table I lists them in free space calculated within two different models. It is already well known that the π - ρ - ω soliton model overestimates the magnetic moments of the nucleon. On the other hand, the results of the traditional charge and magnetization radii of the proton are in good agreement with the experimental data. Note that there is almost no difference between model I and model II in free space, as expected.

If the nucleon is embedded into nuclear medium, then its properties undergo the changes due to the interaction with the surrounding environment. The results listed in Table II demonstrate possible medium modifications of the EM

TABLE I. The electromagnetic properties of the nucleons in free space. The magnetic moments of the proton and the neutron are given in the unit of the nuclear magneton (μ_N).

		Model I	Model II	Experiment
$\langle r_E^2 \rangle_p^{1/2}$	[fm]	0.93	0.93	0.86
$\langle r_M^2 \rangle_p^{1/2}$	[fm]	0.87	0.87	0.78
$\langle r_E^2 \rangle_n$	[fm ²]	-0.23	-0.23	-0.12
$\langle r_M^2 \rangle_n^{1/2}$	[fm]	0.88	0.88	0.86
μ_p	[μ_N]	3.37	3.39	2.79
μ_n	[μ_N]	-2.58	-2.61	-1.91
$ \mu_p/\mu_n $		1.31	1.30	1.46

radii and the magnetic moments of the nucleons at normal nuclear matter density. The size of the proton charge radius in medium turns out to be larger than that in free space. Both the results from Model I and Model II show similar tendencies. It indicates that the nucleon tends to bulge out in nuclear medium. On the other hand, Model I and Model II yield different results. While the neutron charge radius from Model I is almost the same as that in free space, its magnitude from Model II is drastically increased. In fact, the neutron radius is a rather difficult observable to describe theoretically because it comes from the subtraction between the isoscalar and isovector FFs [see Eq. (26)]. As will be discussed later, the traditional charge density of the neutron is very different from the transverse charge density. In addition, the medium effects affect strongly the radial dependence of the neutron charge distribution in comparison with the proton one. Thus, it is difficult to draw any conclusion about the changes of the neutron size in medium, based on the traditional neutron charge density. However, we will soon see that the transverse charge density inside a nucleon will clearly show that both the proton and the neutron swell in nuclear medium. The magnitudes of the magnetic moments of both the proton and the neutron become quite larger in nuclear medium than in free space by approximately 40%, as shown in Table II. The medium effects turn out to be even larger on the neutron magnetic moment than the proton one as observed in the results of their ratio $|\mu_p^*/\mu_n^*|$. The reason can be found in the fact that the magnetization density

TABLE II. The electromagnetic properties of the nucleons in nuclear medium at normal nuclear matter density ρ_0 .

		Model I	Model II
$\langle r_E^{*2} \rangle_p^{1/2}$	[fm]	1.17	1.08
$\langle r_M^{*2} \rangle_p^{1/2}$	[fm]	1.17	1.14
$\langle r_E^{*2} \rangle_n$	[fm ²]	-0.22	-0.40
$\langle r_M^{*2} \rangle_n^{1/2}$	[fm]	1.18	1.17
μ_p^*	[μ_N]	5.23	5.41
μ_n^*	[μ_N]	-4.56	-4.73
$ \mu_p^*/\mu_n^* $		1.15	1.14

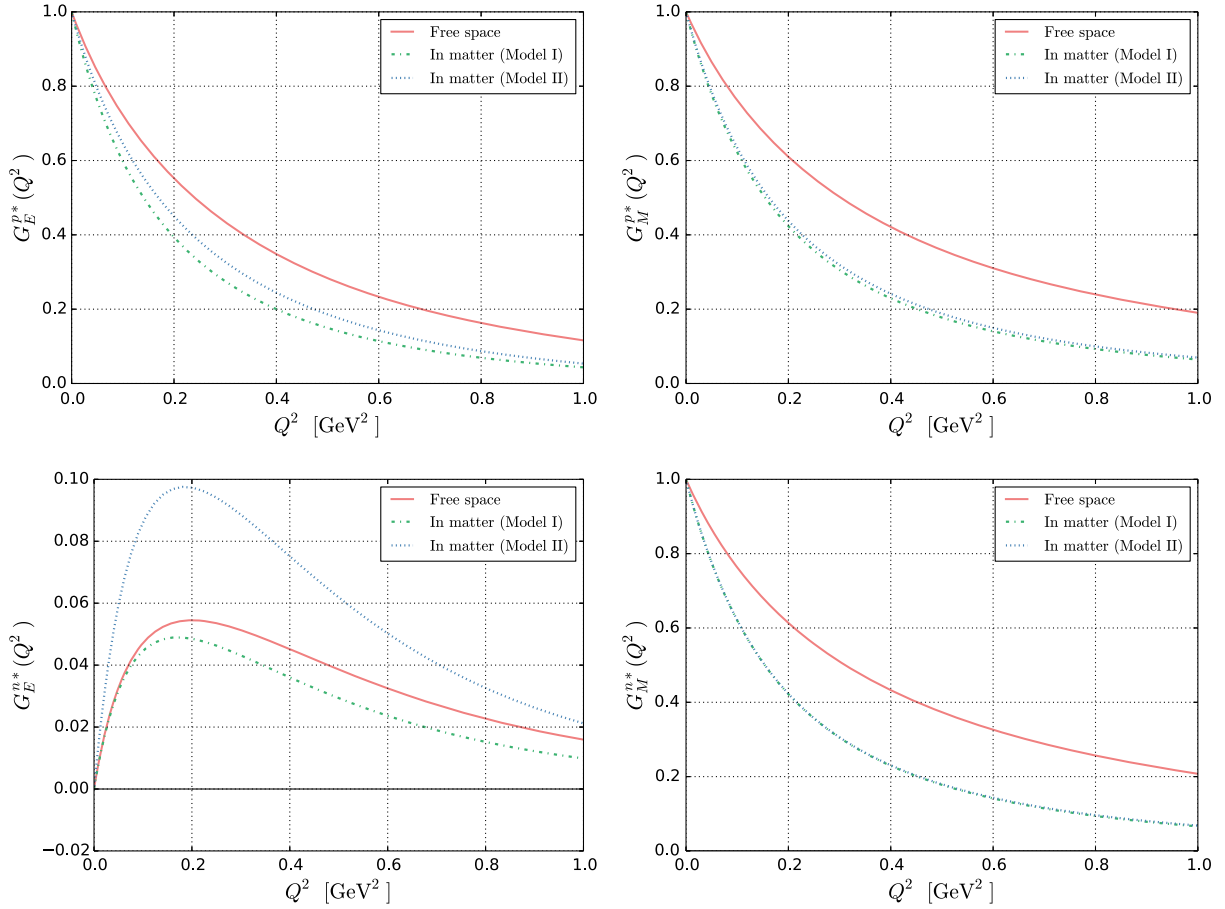


FIG. 1. The electric and magnetic form factors of the proton are drawn respectively in the upper-left and upper-right panels, and those of the neutron are depicted in the lower panels in the same manner as functions of Q^2 . The solid curve represents the form factors in free space, while the dotted and dotted-dashed ones designate, respectively, those from Model I and Model II in nuclear matter.

becomes broadened in medium, which will be shown soon. Since the operator of the magnetic moment is proportional to the distance from the center of the nucleon, the nucleon magnetic moments in general tend to increase in nuclear medium. This also indicates indirectly that the nucleon swells in nuclear matter.

Figure 1 depicts the results for the EMFFs of the proton and the neutron as functions of Q^2 both in free space and in nuclear medium. The EMFFs in free space based on the π - ρ - ω soliton model have been already investigated many years ago [56]. In Ref. [56], it was shown that the electric form factor of both the proton and the neutron are in good agreement even with recent experimental data [57–60]. Since the results for the magnetic moments of the nucleon are quite overestimated within the present model as shown in Table I, the magnitudes of the magnetic form factors are also larger than the data. However, the Q^2 dependence of the magnetic form factors are well explained. The EMFFs have been investigated within various solitonic models [28,61–64]. These chiral soliton approaches describe the Q^2 dependence very well in comparison with the experimental data.

We now discuss the main subject of the present work, i.e., the medium modification of the EMFFs of the nucleon in nuclear matter. As was expected from the charge and magnetic radii of the proton shown in Table II, the EMFFs of the proton in medium fall off faster than those in free space as Q^2 increases. The general tendency of the form factors remains almost unchanged in the case of both Model I and Model II. When it comes to the electric FF of the neutron, however, the result from Model I is very different from that obtained from Model II. We already have seen that Model I and Model II give rather different results for the neutron charge radii. The difference arises from the fact that the ω meson is treated in a distinctive way. In Model I, both the ρ and ω mesons are treated on an equal footing. That is, both the vector mesons undergo changes in the same manner. On the other hand, the ω meson is kept to be the same as in free space in Model II. Since the proton electric FF is given as the sum of the isoscalar and isovector form factors as shown in Eq. (26), the difference between Model I and Model II is marginal (see the results for the electric FFs of the proton in Fig. 1). However, the neutron electric FF comes from the subtraction of the isovector FF

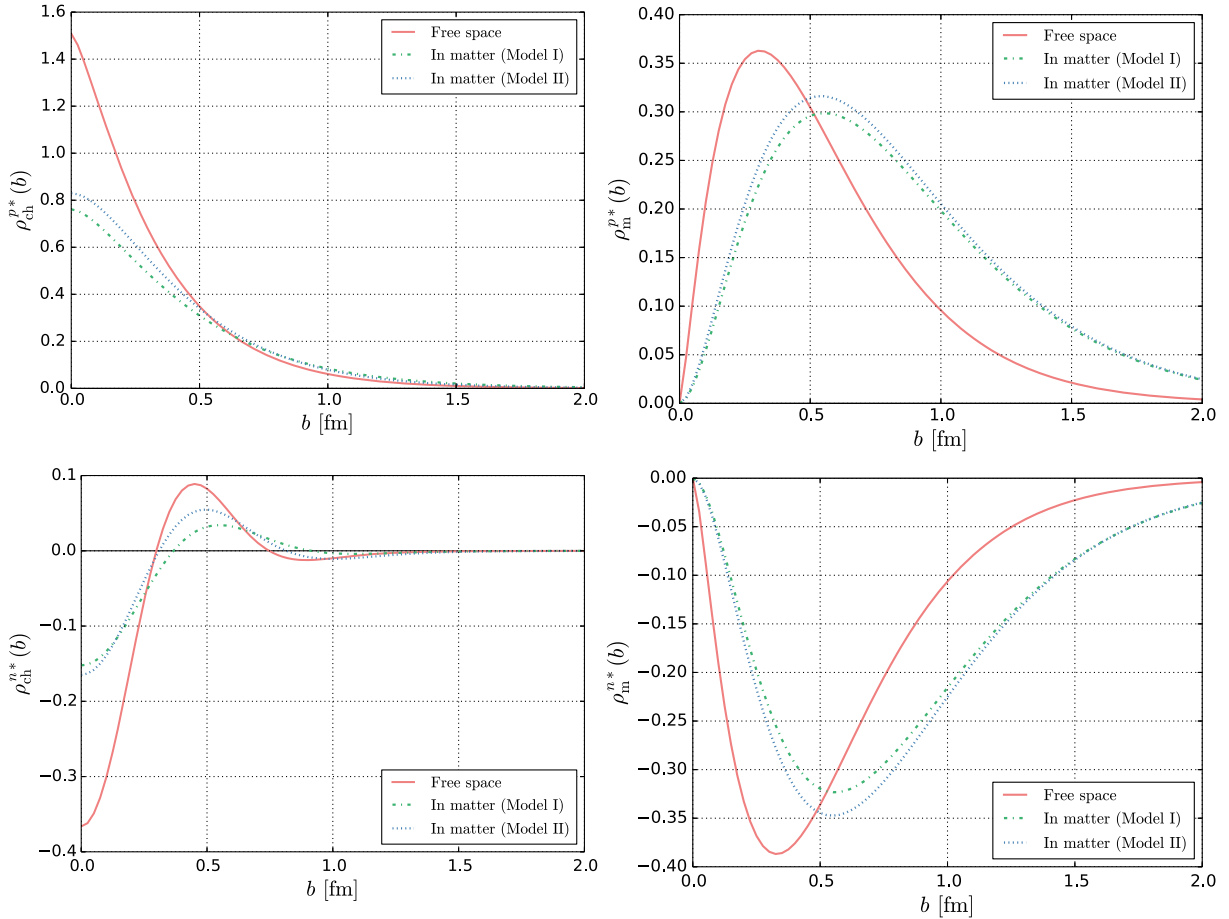


FIG. 2. The transverse charge densities inside an unpolarized proton with $b_x = 0$ are plotted in the upper-left and the upper-right panels, respectively, and those inside a neutron are depicted in the lower panels in the same manner as functions of the impact parameter b . The solid curve represents the transverse densities in free space, while the dotted and dotted-dashed ones designate, respectively, those from Model I and Model II in nuclear matter.

from the isoscalar one. Considering the fact that the ρ meson contributes only to the isovector FF whereas the ω meson comes into play only in the isoscalar FF, we can easily see that the changes of both the ρ and ω mesons are more or less compensated in Model I. However, in Model II, the isoscalar FF remains intact while the isovector FF is modified, which leads to the amplification of the electric FF of the nucleon (see the lower panel of Fig. 1). It is interesting to note that the results for the neutron from Model I is very similar to those from Ref. [39]. Considering the fact that the Skyrme term in Ref. [39] is related to the vector mesons by the resonance saturation [65], The characteristics of Model I are closer to the medium-modified Skyrme model in which both the pion kinetic and Skyrme terms are modified, compared to Model II.

The results for the transverse charge and magnetization distributions inside an unpolarized proton are drawn in the upper-left and upper-right panels, respectively, with $b_x = 0$. The medium-modified transverse charge densities near the center of the proton are reduced drastically but get larger as b increases. It indicates that the transverse size of

the nucleon becomes larger in nuclear medium. As for the transverse magnetization densities, we find that the densities in medium are shifted and broadened in comparison with that in free space. It also implies that the in-medium nucleon swells relatively to the free space one.

It is already well known that the transverse charge density inside an unpolarized neutron provides a new aspect on the structure of the neutron [25,54]. Considering the fact that the transverse charge density inside a nucleon has a physical meaning of the probability of finding a quark inside a nucleon, we can see from the results for the transverse charge densities inside a neutron, which are depicted in the lower-left panel of Fig. 2, that the negative charged quarks, i.e. down quarks are more probably found in the vicinity of the center of the neutron whereas the positive charged quarks or up quarks are located in outer regions inside a neutron. This is very much different from the usual and traditional understanding of the neutron charge distribution in which the positive charge is found near the center of the neutron while the negative charge is placed in outer regions. In nuclear matter, the transverse charge density inside a neutron

TABLE III. The transverse charge and magnetization radii of the unpolarized proton and the neutron. The results in free space and in nuclear matter at normal nuclear matter density, ρ_0 , are presented.

		Free space	Model I	Model II
$\langle b_{\text{ch}}^2 \rangle_p^{1/2}$	[fm]	0.70	0.90	0.81
$\langle b_{\text{m}}^2 \rangle_p^{1/2}$	[fm]	0.89	1.65	1.67
$\langle b_{\text{ch}}^2 \rangle_n$	[fm ²]	-0.023	-0.015	-0.042
$\langle b_{\text{m}}^2 \rangle_n$	[fm ²]	-0.85	-2.89	-2.89

has the same tendency but the magnitude of the densities is reduced and is broadened, as shown in the lower-left panel of Fig. 2. It implies that the size of the neutron is also extended in nuclear medium. The transverse magnetization density inside a neutron is similarly modified in nuclear medium as that inside a proton.

To see the swelling of the nucleon in nuclear matter more clearly, we define the transverse mean square charge and magnetization radii of the nucleon as follows

$$\langle b_{\text{ch,m}}^2 \rangle_{p,n} = \int d^2b b^2 \rho_{\text{ch,m}}^{p,n}(b), \quad (34)$$

where the transverse charge density, ρ_{ch} , and the transverse magnetization density, ρ_{m} are defined in Eq. (28) and Eq. (29), respectively. The results for the transverse charge and magnetization radii of the proton and the neutron are listed in Table III. The transverse mean square charge radius of the proton in nuclear medium is increased approximately by 20%. On the other hand, the medium-modified transverse mean magnetization radius of the proton becomes almost twice as large as that in free space. In the case of the neutron, the result from Model I shows slightly smaller than that in free space whereas the result from Model II is almost about two times larger than that in free

space. As we have already discussed previously, the role of the ω meson becomes much more influential in the case of the neutron than in the proton case.

We are now in a position to discuss the results for the transverse charge density when the nucleon is polarized. As shown in Eq. (31), the transverse charge density inside a polarized nucleon becomes deviated from that inside an unpolarized nucleon by the second term of the right-hand side of Eq. (31). Figure 3 shows the general feature of the transverse charge densities inside both the polarized proton (upper-left panel) and the polarized neutron (upper-right panel). As was already discussed in Ref. [26], the magnetic field that makes the nucleon polarized along the x axis produces an induced electric field along the y axis according to Einstein's theory of special relativity [66]. As a result, the transverse charge density inside both the polarized proton is distorted and shifted in the direction of the negative y axis. In the case of the neutron, the distortion of the corresponding density is complicated, since the anomalous magnetic moment of the neutron is negative and the transverse charge density inside an unpolarized neutron has a different feature, compared with the proton case. Thus, the negative charged quarks inside a neutron is shifted to the positive y axis and the positive charged quarks is displaced to the positive y axis, revealing an asymmetric distortion.

Figure 4 illustrates the medium modification of the transverse charge densities inside both the polarized proton and neutron. The general behavior of the transverse charge densities in nuclear medium is very similar to those in free space. However, the extension of the nucleon size is observed in nuclear medium. Examining the results shown in Fig. 4 the effects due to the polarization of the nucleon are lessened in nuclear medium. This can be understood from the medium modification of the transverse charge and magnetization densities inside an unpolarized nucleon as shown in Fig. 2. These densities in medium indicate that the

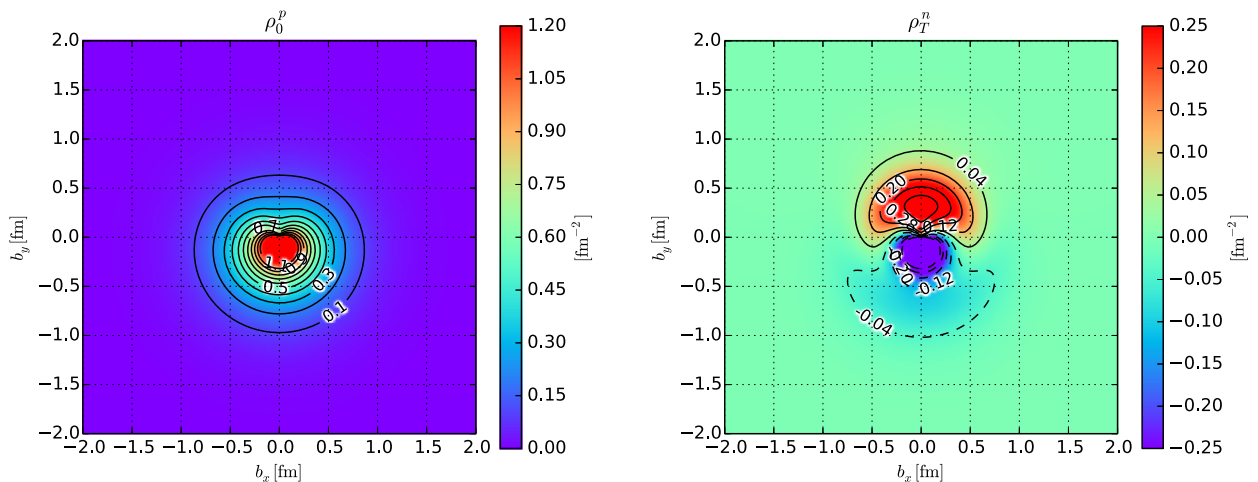


FIG. 3. Transverse charge densities inside the polarized proton (left panel) and neutron (right panel) in free space.

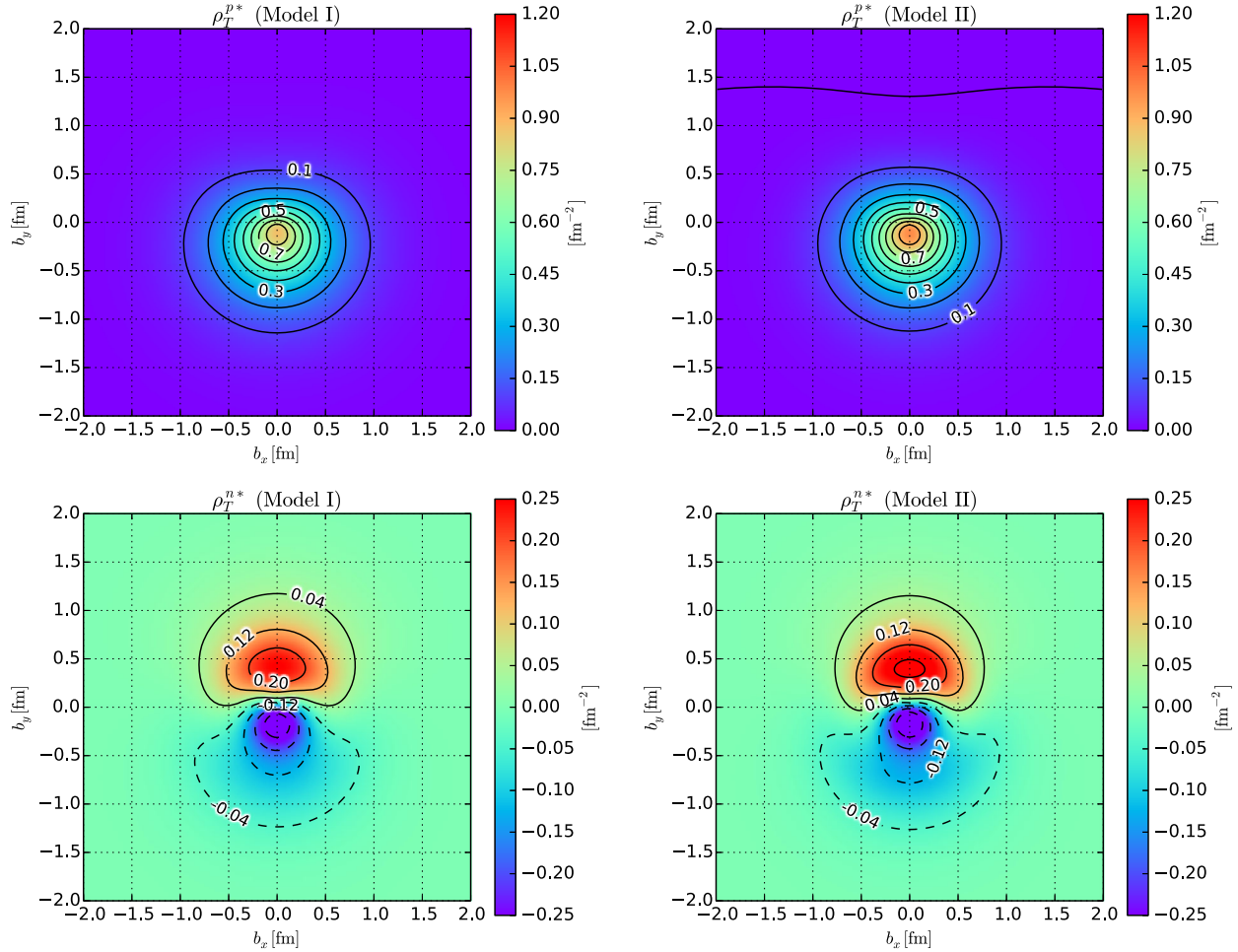


FIG. 4. Transverse charge densities inside the polarized proton (upper panels) and neutron (lower panels) in nuclear medium at normal nuclear matter density ρ_0 from Model I (left panels) and Model II (right panels), respectively.

size of the nucleon in medium becomes larger and the effects of the polarization also get diminished.

B. EMT form factors and transverse energy-momentum densities

Let us now discuss the EMTFFs of the nucleon. Since the EMTFFs correspond to the generalized isoscalar VFFs, We do not need to distinguish the proton from the neutron. The same results hold for the nucleon embedded into isospin-symmetric nuclear matter. The situation will change if one introduces the effects of isospin breaking into the mesonic sector. When one considers more realistic isospin asymmetric nuclear matter, one has to compute both the isoscalar and isovector generalized vector FFs. In this case, the EMTFFs will be regarded only as a part of the GVFFs. In the present work, we concentrate only on isospin-symmetric nuclear medium.

The medium-modified EMTFFs of the nucleon have been already investigated in Ref. [46] in detail. Thus, we will discuss here only the transverse charge and magnetization

densities inside a nucleon, which correspond to the EMTFFs. As shown in Eq. (18), the EMTFFs of the nucleon are identified as the GVFFs in the NLO, which arise from the second moments of the vector GPDs. Hence, the transverse charge and magnetization densities from the EMTFFs of the nucleon can be regarded as those inside a nucleon to the NLO.

Figure 5 draws the NLO transverse charge densities inside both the unpolarized nucleon (left panel), ρ_{20}^* and the polarized nucleon (right panel), $\rho_{20,T}^*$, with b_x fixed to be zero. Interestingly, the general feature of ρ_{20}^* is almost the same as ρ_{ch}^p presented in Fig. 2. When the nucleon is polarized, the $\rho_{20,T}$ is changed drastically, as shown in the right panel of Fig. 5. However, it can be also easily understood as we have discussed previously. The induced electric field will cause the shift of the positive charged quark to the negative y direction whereas will translate the negative one to the positive y axis. The strengths of the NLO transverse charge densities are much decreased in nuclear medium. In particular, the magnitude of the negative charge is almost suppressed. Figure 6 depicts

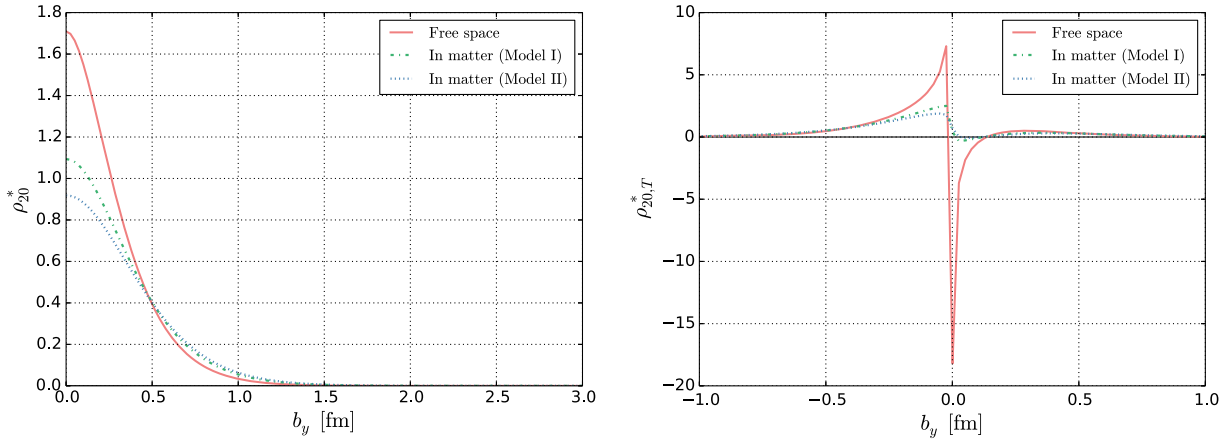


FIG. 5. The NLO transverse charge densities inside the unpolarized nucleon, ρ_{20}^* , in the left panel, and those inside the polarized nucleon, $\rho_{20,T}^*$, in the right panel, with $b_x = 0$. The solid curve depicts those in free space, while the dotted and dotted-dashed ones represent, respectively, those from model I and model II in nuclear matter.

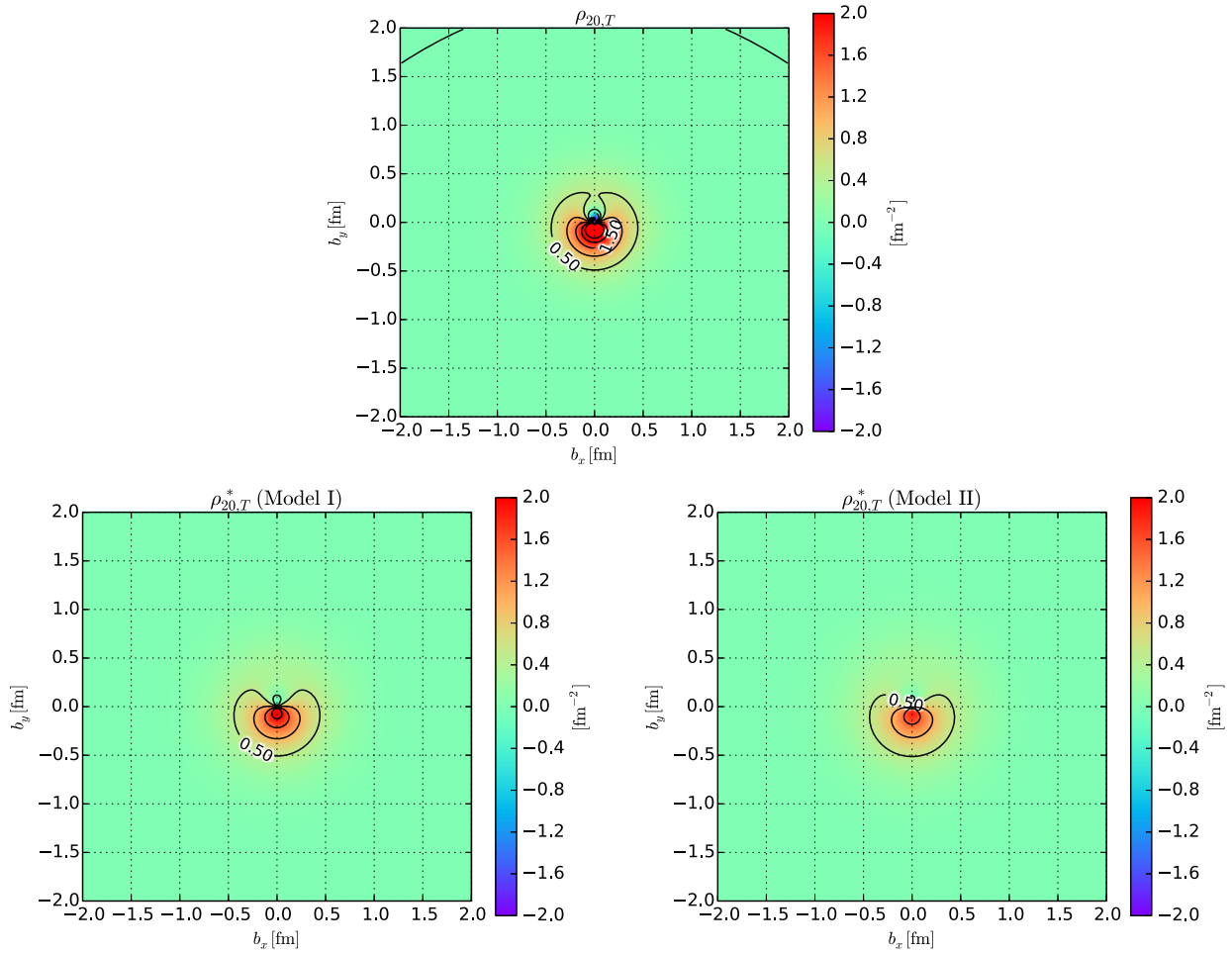


FIG. 6. The two-dimensional NLO transverse charge densities inside the polarized nucleon in free space, $\rho_{20,T}$, (upper panel), and those inside the polarized nucleon, $\rho_{20,T}^*$, (lower panel). The lower-left panel depicts $\rho_{20,T}^*$ from Model I and the lower-right panel draws those from Model II.

the two-dimensional transverse charge densities inside the polarized nucleon both in free space and in nuclear matter. The results show clearly the polarization effects of the nucleon on the transverse charge densities, as in the right panel of Fig. 5.

V. SUMMARY AND OUTLOOK

In the present work, we investigated the electromagnetic form factors of the nucleon in nuclear medium, based on the π - ρ - ω soliton model. We employed two different models: Model I was constructed by changing both the ρ meson and the ω meson in nuclear matter, while in Model II only the ρ meson undergoes the change but the ω meson is intact. This difference yielded the very different results for the neutron electric form factor. We also discussed the transverse charge and magnetization densities inside both the unpolarized nucleon and the polarized nucleon. The densities showed that the nucleon swells in nuclear matter, which was also the case in the medium-modified Skyrme model. The effects of the nucleon polarization turned out to be lessened in nuclear matter. Finally, we presented the results for the next-to-leading

order transverse charge densities obtained from the energy-momentum tensor form factors or the generalized vector form factors of the nucleon.

Based on the π - ρ - ω soliton model, it is also of great interest to study the spin problem of the nucleon, in particular, the spin densities of the nucleon [67]. While the model does not contain any quark degrees of freedom, it is still possible to study the quark spin distributions inside a nucleon. The present work will shed light on the spin structure of the nucleon from a complementary viewpoint and furthermore on the changes of its spin structure in nuclear medium. The corresponding work is under way.

ACKNOWLEDGMENTS

This work is supported by the Basic Science Research Program through the National Research Foundation (NRF) of Korea funded by the Korean government (Ministry of Education, Science and Technology), Grant No. 2011-0023478 (J.H.J. and U.Y.) and NRF-2013S1A2A203 5612 (H.Ch.K.). J. H. J. also acknowledges a partial support by the ‘‘Fonds zur F6rderung der wissenschaftlichen Forschung in 6sterreich via FWF DK W1203-N16’’.

-
- [1] M. K. Jones *et al.* (Jefferson Lab Hall A Collaboration), G_{E_p}/G_{M_p} ratio by polarization transfer in $\vec{e}p \rightarrow e\vec{p}$, *Phys. Rev. Lett.* **84**, 1398 (2000).
- [2] O. Gayou *et al.* (Jefferson Lab Hall A Collaboration), Measurements of the elastic electromagnetic form-factor ratio $\mu_p G_{E_p}/G_{M_p}$ via polarization transfer, *Phys. Rev. C* **64**, 038202 (2001).
- [3] O. Gayou *et al.* (Jefferson Lab Hall A Collaboration), Measurement of G_{E_p}/G_{M_p} in $\vec{e}p \rightarrow e\vec{p}$ to $Q^2 = 5.6\text{GeV}^2$, *Phys. Rev. Lett.* **88**, 092301 (2002).
- [4] V. Punjabi *et al.* (Jefferson Lab Hall A Collaboration), Proton elastic form-factor ratios to $Q^2 = 3.5\text{GeV}^2$ by polarization transfer, *Phys. Rev. C* **71**, 055202 (2005); **71**, 069902(E) (2005).
- [5] A. J. R. Puckett *et al.*, Recoil Polarization Measurements of the Proton Electromagnetic Form Factor Ratio to $Q^2 = 8.5\text{GeV}^2$, *Phys. Rev. Lett.* **104**, 242301 (2010).
- [6] J. C. Bernauer *et al.* (A1 Collaboration), High-Precision Determination of the Electric and Magnetic Form Factors of the Proton, *Phys. Rev. Lett.* **105**, 242001 (2010).
- [7] G. Ron *et al.* (Jefferson Lab Hall A Collaboration), Low Q^2 measurements of the proton form factor ratio $\mu_p G_E/G_M$, *Phys. Rev. C* **84**, 055204 (2011).
- [8] X. Zhanl *et al.*, High precision measurement of the proton elastic form factor ratio $\mu_p G_E/G_M$ at low Q^2 , *Phys. Lett. B* **705**, 59 (2011).
- [9] A. J. R. Puckett *et al.*, Final analysis of proton form factor ratio data at $Q^2 = 4.0, 4.8, \text{ and } 5.6\text{GeV}^2$, *Phys. Rev. C* **85**, 045203 (2012).
- [10] B. S. Schlimme *et al.*, Measurement of the Neutron Electric to Magnetic Form Factor Ratio at $Q^2 = 1.58\text{GeV}^2$ Using the Reaction ${}^3\text{He}(\vec{e}, e'n)pp$, *Phys. Rev. Lett.* **111**, 132504 (2013).
- [11] J. C. Bernauer *et al.* (A1 Collaboration), Electric and magnetic form factors of the proton, *Phys. Rev. C* **90**, 015206 (2014).
- [12] C. E. Hyde-Wright and K. de Jager, Electromagnetic form factors of the nucleon and Compton scattering, *Annu. Rev. Nucl. Part. Sci.* **54**, 217 (2004).
- [13] J. Arrington, C. D. Roberts, and J. M. Zanotti, Nucleon electromagnetic form-factors, *J. Phys. G* **34**, S23 (2007).
- [14] C. F. Perdrisat, V. Punjabi, and M. Vanderhaeghen, Nucleon electromagnetic form factors, *Prog. Part. Nucl. Phys.* **59**, 694 (2007).
- [15] S. Pacetti, R. Baldini Ferroli, and E. Tomasi-Gustafsson, Proton electromagnetic form factors: Basic notions, present achievements and future perspectives, *Phys. Rep.* **550–551**, 1 (2015).
- [16] D. M6ller, D. Robaschik, B. Geyer, F.-M. Dittes, and J. Hořejši, Wave functions, evolution equations and evolution kernels from light ray operators of QCD, *Fortschr. Phys.* **42**, 101 (1994).
- [17] X. D. Ji, Gauge Invariant Decomposition of Nucleon Spin, *Phys. Rev. Lett.* **78**, 610 (1997).
- [18] X. D. Ji, Deeply-virtual Compton scattering, *Phys. Rev. D* **55**, 7114 (1997).
- [19] A. V. Radyushkin, Scaling limit of deeply virtual Compton scattering, *Phys. Lett. B* **380**, 417 (1996).

- [20] K. Goeke, M. V. Polyakov, and M. Vanderhaeghen, Hard exclusive reactions and the structure of hadrons, *Prog. Part. Nucl. Phys.* **47**, 401 (2001).
- [21] M. Diehl, Generalized parton distributions, *Phys. Rep.* **388**, 41 (2003).
- [22] A. V. Belitsky and A. V. Radyushkin, Unraveling hadron structure with generalized parton distributions, *Phys. Rep.* **418**, 1 (2005).
- [23] M. Burkardt, Impact parameter space interpretation for generalized parton distributions, *Int. J. Mod. Phys. A* **18**, 173 (2003).
- [24] M. Burkardt, Impact parameter dependent parton distributions and off forward parton distributions for $\rightarrow \zeta^0$, *Phys. Rev. D* **62**, 071503 (2000); **66**, 119903(E) (2002).
- [25] G. Miller, Charge Densities of the Neutron and Proton, *Phys. Rev. Lett.* **99**, 112001 (2007).
- [26] C. E. Carlson and M. Vanderhaeghen, Empirical Transverse Charge Densities in the Nucleon and the Nucleon-to-Delta Transition, *Phys. Rev. Lett.* **100**, 032004 (2008).
- [27] A. Silva, D. Urbano, and H.-Ch. Kim, Flavour structure of the nucleon electromagnetic form factors and transverse charge densities in the chiral quark-soliton model, [arXiv:1305.6373](https://arxiv.org/abs/1305.6373).
- [28] H.-Ch. Kim, A. Silva, and D. Urbano, Flavor structure of the nucleon electromagnetic form factors, *J. Phys. Soc. Jpn. Conf. Proc.* **1**, 013039 (2014).
- [29] D. Chakrabarti and C. Mondal, Transverse charge and magnetization densities in holographic QCD, *Eur. Phys. J. C* **74**, 2962 (2014).
- [30] D. Chakrabarti, C. Mondal, and A. Mukherjee, Gravitational form factors and transverse spin sum rule in a light front quark-diquark model in AdS/QCD, *Phys. Rev. D* **91**, 114026 (2015).
- [31] S. Malace, M. Paolone, and S. Strauch (Jefferson Lab Hall A Collaboration), Medium modifications from ${}^4\text{He}(\vec{e}, e', \vec{P})$, *AIP Conf. Proc.* **1056**, 141 (2008).
- [32] S. Dieterich, P. Bartsch, D. Baumann, J. Bermuth, K. Bohinc, R. Bohm, D. Bosnar, S. Derber *et al.*, Polarization transfer in the ${}^4\text{He}(\vec{e}, e', \vec{P})^3$ reaction, *Phys. Lett. B* **500**, 47 (2001).
- [33] H. Avakian *et al.* (CLAS Collaboration), Measurement of beam-spin asymmetries for π^+ electroproduction above the baryon resonance region, *Phys. Rev. D* **69**, 112004 (2004).
- [34] S. Strauch *et al.* (Jefferson Lab E93-049 Collaboration), Polarization Transfer in the ${}^4\text{He}(\vec{e}, e', \vec{P})^3\text{H}$ Reaction up to $Q^2 = 2.6 - (\text{GeV}/c)^2$, *Phys. Rev. Lett.* **91**, 052301 (2003).
- [35] D.-H. Lu, K. Tsushima, A. W. Thomas, A. G. Williams, and K. Saito, Electromagnetic form-factors of the bound nucleon, *Phys. Rev. C* **60**, 068201 (1999).
- [36] J. R. Smith and G. A. Miller, Chiral solitons in nuclei: Electromagnetic form-factors, *Phys. Rev. C* **70**, 065205 (2004).
- [37] I. C. Cloet, G. A. Miller, E. Piassetzky, and G. Ron, Neutron Properties in the Medium, *Phys. Rev. Lett.* **103**, 082301 (2009).
- [38] U. T. Yakhshiev, U.-G. Meissner, and A. Wirzba, Electromagnetic form-factors of bound nucleons revisited, *Eur. Phys. J. A* **16**, 569 (2003).
- [39] U. Yakhshiev and H.-Ch. Kim, Properties of the bound nucleons, *Eur. Phys. J. Web Conf.* **20**, 04005 (2012).
- [40] A. Airapetian *et al.* (HERMES Collaboration), Nuclear-mass dependence of azimuthal beam-helicity and beam-charge asymmetries in deeply virtual Compton scattering, *Phys. Rev. C* **81**, 035202 (2010).
- [41] A. Rakhimov, M. M. Musakhanov, F. C. Khanna, and U. T. Yakhshiev, Medium modification of nucleon properties in Skyrme model, *Phys. Rev. C* **58**, 1738 (1998).
- [42] U. Yakhshiev and H.-Ch. Kim, Binding energy per nucleon and hadron properties in nuclear matter, *Phys. Rev. C* **83**, 038203 (2011).
- [43] C. Cebulla, K. Goeke, J. Ossmann, and P. Schweitzer, The nucleon form-factors of the energy momentum tensor in the Skyrme model, *Nucl. Phys.* **A794**, 87 (2007).
- [44] J.-H. Jung, U. T. Yakhshiev, and H. -Ch. Kim, Energy-momentum tensor form factors of the nucleon within a π - ρ - ω soliton model, *J. Phys. G* **41**, 055107 (2014).
- [45] H. -Ch. Kim, P. Schweitzer, and U. Yakhshiev, Energy-momentum tensor form factors of the nucleon in nuclear matter, *Phys. Lett. B* **718**, 625 (2012).
- [46] J. H. Jung, U. Yakhshiev, H. -Ch. Kim, and P. Schweitzer, In-medium modified energy-momentum tensor form factors of the nucleon within the framework of a π - ρ - ω soliton model, *Phys. Rev. D* **89**, 114021 (2014).
- [47] J.-H. Jung, U. T. Yakhshiev, and H. -Ch. Kim, In-medium modified π - ρ - ω mesonic Lagrangian and properties of nuclear matter, *Phys. Lett. B* **723**, 442 (2013).
- [48] U.-G. Meissner and N. Kaiser, Massive yang-mills approach to Skyrmions with vector mesons, *Z. Phys. A* **325**, 267 (1986).
- [49] T. Ericson and W. Weise, *Pions and Nuclei* (Clarendon, Oxford, 1988).
- [50] M. Naruki *et al.* (KEK-PS E325 Collaboration), Experimental signature of the medium modification for rho and omega mesons in 12-GeV $p + A$ reactions, *Phys. Rev. Lett.* **96**, 092301 (2006).
- [51] M. H. Wood *et al.* (CLAS Collaboration), Light vector mesons in the nuclear medium, *Phys. Rev. C* **78**, 015201 (2008).
- [52] M. V. Polyakov, Generalized parton distributions and strong forces inside nucleons and nuclei, *Phys. Lett. B* **555**, 57 (2003).
- [53] J. J. Kelly, Nucleon charge and magnetization densities from Sachs form-factors, *Phys. Rev. C* **66**, 065203 (2002).
- [54] G. A. Miller, Transverse charge densities, *Annu. Rev. Nucl. Part. Sci.* **60**, 1 (2010).
- [55] S. Venkat, J. Arrington, G. A. Miller, and X. Zhan, Realistic transverse images of the proton charge and magnetic densities, *Phys. Rev. C* **83**, 015203 (2011).
- [56] U.-G. Meissner, N. Kaiser, and W. Weise, Nucleons as Skyrme solitons with vector mesons: Electromagnetic and axial properties, *Nucl. Phys.* **A466**, 685 (1987).
- [57] C. Herberg *et al.*, Determination of the neutron electric form-factor in the $D(e, e', n)p$ reaction and the influence of nuclear binding, *Eur. Phys. J. A* **5**, 131 (1999).
- [58] J. Bermuth *et al.*, The neutron charge form-factor and target analyzing powers from ${}^3\text{He}(\vec{e}, e', n)$ scattering, *Phys. Lett. B* **564**, 199 (2003).
- [59] D. I. Glazier *et al.*, Measurement of the electric form-factor of the neutron at $Q^2 = 0.3 - (\text{GeV}/c)^2$ to $0.8 - (\text{GeV}/c)^2$, *Eur. Phys. J. A* **24**, 101 (2005).
- [60] B. Plaster *et al.* (Jefferson Laboratory E93-038 Collaboration), Measurements of the neutron electric to magnetic

- form-factor ratio G_{En}/G_{Mn} via the ${}^2\text{H}(\bar{e}, e', \bar{n}){}^1\text{H}$ reaction to $Q^2 = 1.45 - (\text{GeV}/c)^2$, *Phys. Rev. C* **73**, 025205 (2006).
- [61] G. Holzwarth, Electromagnetic nucleon form-factors and their spectral functions in soliton models, *Z. Phys. A* **356**, 339 (1996).
- [62] H. Weigel, Chiral soliton models for baryons, *Lect. Notes Phys.* **743**, 1 (2008).
- [63] H.-Ch. Kim, A. Blotz, M. V. Polyakov, and K. Goeke, Electromagnetic form-factors of the SU(3) Octet baryons in the semibosonized SU(3) Nambu-Jona-Lasinio model, *Phys. Rev. D* **53**, 4013 (1996).
- [64] C. V. Christov, A. Blotz, H.-Ch. Kim, P. Pobylitsa, T. Watabe, T. Meissner, E. Ruiz Arriola, and K. Goeke, Baryons as nontopological chiral solitons, *Prog. Part. Nucl. Phys.* **37**, 91 (1996).
- [65] G. Ecker, J. Gasser, A. Pich, and E. de Rafael, The role of resonances in chiral perturbation theory, *Nucl. Phys.* **B321**, 311 (1989).
- [66] A. Einstein, On the electrodynamics of moving bodies, *Ann. Phys. (Berlin)* **322**, 891 (1905).
- [67] M. Diehl and Ph. Hagler, Spin densities in the transverse plane and generalized transversity distributions, *Eur. Phys. J. C* **44**, 87 (2005).